

# Crystal Research and Technology

Journal of Experimental and Industrial Crystallography



Numerical modelling of instability and supercritical oscillatory states in a Czochralski model system of oxide melts

(N. Crnogorac, H. Wilke, K. A. Cliffe, A. Yu. Gelfgat, and E. Kit, p. 606)



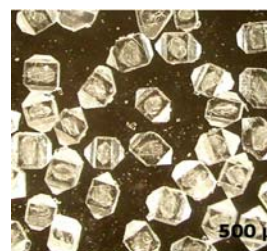
## COVER PICTURE

The cover picture shows a DyScO<sub>3</sub> crystal with an extreme case of spiral growth (left) and an SmScO<sub>3</sub> crystal with very distinctive spiral growth (right). (see pages 606 – 615).

## ORIGINAL PAPERS

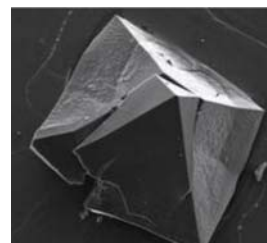
- Page **583–587** \_\_\_\_\_ Guozong Zheng, Jingkui Liang, Zhengdong Li, Genbo Su, and Xinxin Zhuang  
The combined effects of supersaturation and Ba<sup>2+</sup> on the batch cooling crystallization of potassium dihydrogen phosphate

The combined effects of supersaturation and Ba<sup>2+</sup> on potassium dihydrogen phosphate (KDP) were investigated in batch cooling suspension crystallization. Growth size, morphology, and impurity Ba<sup>2+</sup> adsorbed in the KDP crystals were measured with changing Ba<sup>2+</sup> concentration and supersaturation. Significant changes in shapes and volume of the grown crystals have been observed. The results further confirmed that the size ...



- Page **588–593** \_\_\_\_\_ F. Hodzhaoglu, F. Kurniawan, V. Mirsky, and C. Nanev  
Gold nanoparticles induce protein crystallization

Nucleation of protein crystals by gold nanoparticles was observed. Lysozyme and ferritin were used as model proteins. The effect was established with uncoated gold nanoparticles and with gold nanoparticles coated by 16-mercaptopalmitic acid.



Page **594–598** \_\_\_\_\_ A. G. Kunjomana and K. A. Chandrasekharan

### Dislocation and microindentation analysis of vapour grown $\text{Bi}_2\text{Te}_{3-x}\text{Se}_x$ whiskers

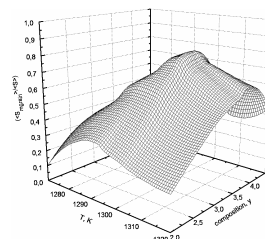
The structural defects and microhardness of  $\text{Bi}_2\text{Te}_{3-x}\text{Se}_x$  whiskers ( $x = 0, 0.2$  and  $0.4$  at % Se) grown by physical vapour deposition (PVD) method have been investigated. Concentric pairs of dislocation loops were observed on the as-grown surfaces of short hexagonal prisms. A systematic study of dislocations in these crystals was carried out by chemical etching ...



Page **599–605** \_\_\_\_\_ N. A. Kalanda, L. I. Gurskii, A. M. Saad, V. M. Truhan, and T. V. Haliakovich

### Crystallization features of $\text{YBa}_2\text{Cu}_3\text{O}_{7-\delta}$ in the $\text{Y}_2\text{BaCuO}_5$ - $\text{BaCuO}_2$ - $\text{CuO}$ and $\text{Y}_2\text{Cu}_2\text{O}_5$ - $\text{BaCuO}_2$ systems

Based on the data of X-ray phase and microstructure analysis, the sample composition was optimized in order to provide maximum size of the textured macrograins of  $\text{YBa}_2\text{Cu}_3\text{O}_{7-\delta}$  and of the crystallites in the  $\text{Y}_2\text{BaCuO}_5$ - $\text{BaCuO}_2$ - $\text{CuO}$ ,  $\text{Y}_2\text{Cu}_2\text{O}_5$ - $\text{BaCuO}_2$  systems. The growth rate has been studied and the  $\text{YBa}_2\text{Cu}_3\text{O}_{7-\delta}$  growth activation energy has been calculated for the samples of ...



Page **606–615** \_\_\_\_\_ N. Crnogorac, H. Wilke, K. A. Cliffe, A. Yu. Gelfgat, and E. Kit

### Numerical modelling of instability and supercritical oscillatory states in a Czochralski model system of oxide melts

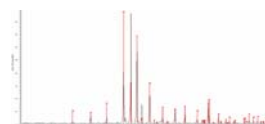
The motivation for this study is the need for accurate numerical models of melt flow instabilities during Czochralski growth of oxides. Such instabilities can lead to undesirable spiralling shapes of the bulk crystals produced by the growing process. The oxide melts are characterized by Prandtl numbers in the range  $5 < Pr < 20$ , which makes the oxide melt flow qualitatively different from the intensively studied ...



Page **616–625** \_\_\_\_\_ T. A. Graber, J. W. Morales, P. A. Robles, H. R. Galleguillos, and M. E. Taboada

### Behavior of $\text{LiOH}\cdot\text{H}_2\text{O}$ crystals obtained by evaporation and by drowning out

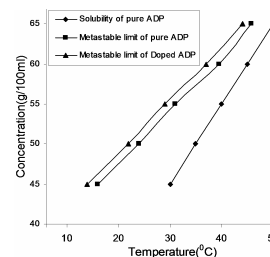
In the present work, the behavior of crystals derived from two different crystallization methods applied in a concentrated aqueous lithium salt solution was studied. The  $\text{LiOH}\cdot\text{H}_2\text{O}$  crystals obtained by a simple evaporation (Crystal I) differed in terms of ...



Page 626–633 \_\_\_\_\_ G. Anandha Babu and P. Ramasamy

### Effect of additives in supersaturated binary and ternary solutions on cluster growth by gravity driven concentration gradient studies

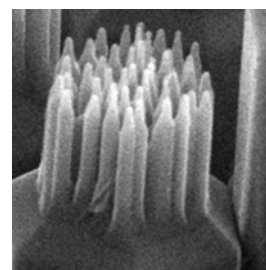
The concentration gradients formed in long column supersaturated solutions of the binary systems Potassium dihydrogen phosphate - Water, Benzophenone - Ethanol, Ammonium dihydrogen phosphate – Water, Potassium hydrogen phthalate – Water and ternary systems Potassium dihydrogen phosphate – Potassium chloride - Water, Benzophenone – Urea - Ethanol, Ammonium dihydrogen phosphate ...



Page 634–639 \_\_\_\_\_ Jing Xiao, Wei Zhang, Yue Wu, and Hui Sun

### Controlled growth of ZnO torch-like nanostructure arrays

Single-crystal ZnO torch-like nanostructure arrays were synthesized using a simple two-step pressure controlled thermal evaporation method without any catalyst. The nanostructures had a hierarchical morphology, with well-hexagonal faceted holders and needle-like flames on them. The diameter of each single flame was about 20-40nm at the base and 10nm at the tip. Both the holders and flames were found to grow along the ...



Page 640–644 \_\_\_\_\_ A. Ruban Kumar and S. Kalainathan

### Growth and characterization of nano-crystalline hydroxyapatite at physiological conditions

Pure, stable stoichiometric nano crystalline hydroxyapatite material was crystallized by double diffusion technique at physiological conditions, temperature at 37°C and pH at 7.4. The sample was sintered at 400°C, 750°C and 1200°C with equal interval of time. They were characterized by X-ray diffraction studies, Fourier Transformation Infra-Red analysis, Thermogravimetric analysis, Scanning Electron Microscopic studies and Atomic Force ...



Page 645–650 \_\_\_\_\_ D. Kalaiselvi, R. Mohan Kumar, and R. Jayavel

### Growth, optical and thermal studies of nonlinear optical L-arginine perchlorate single crystals

A potentially useful semiorganic nonlinear optical (NLO) material, L-arginine perchlorate, has been synthesized and bulk crystals have been grown by slow cooling technique. The grown crystals were characterized by single crystal X-ray diffraction, ...



Page **651–655** \_\_\_\_\_ X. F. Chen, D. Siche, M. Albrecht, C. Hartmann, J. Wollweber, and X. G. Xu

### Surface preparation of AlN substrates

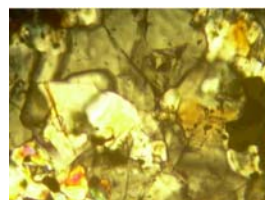
The Al-polar surfaces of AlN wafers cut from physical vapor transport grown crystals were lapped and polished. Polishing procedures were developed to produce surfaces for epitaxial growth. The surface scratches and subsurface damage caused by mechanical polishing were removed by a final ...



Page **656–665** \_\_\_\_\_ M. Szurgot, K. Polański, and M. Krystek

### Electron and optical microscopy studies of extraterrestrial minerals in NWA4047 meteorite

Analytical electron microscopy and optical microscopy were used to determine the elemental and mineral composition of NWA4047 meteorite. The meteorite was found in 2005 in Morocco, and in 2006 was preliminary classified as H4-5 ordinary chondrite. The main crystalline meteorite minerals: olivines, pyroxenes, kamacite and taenite, feldspars, ...



Page **666–669** \_\_\_\_\_ Min Jin, Jiayue Xu, Aiyong Wu, Xinhua Li, Hui Shen, and Qingbo He

### Investigation of domain structures in PZNT93/7 crystals by chemical etching

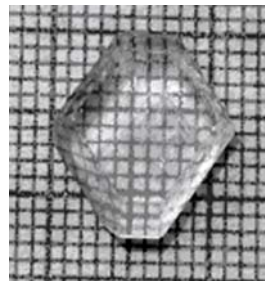
The domain structures in  $0.93\text{Pb}(\text{Zn}_{1/3}\text{Nb}_{2/3})\text{O}_3$ - $0.07\text{PbTiO}_3$  (PZNT93/7) crystals were investigated by chemical etching technique. Original antiparallel  $180^\circ$  domains of size 20–40  $\mu\text{m}$  were observed on the surface of as-grown PZNT93/7 crystal. It was found the domain states are sensitive to the stress field induced by mechanical processing or impurities. As the composition of PZNT93/7 crystal was located near the morphotropic phase boundary, various ...



Page **670–673** \_\_\_\_\_ S. Krishnan, C. Justin Raj, S. Dinakaran, and S. Jerome Das

### Investigation of optical band gap in potassium acid phthalate single crystal

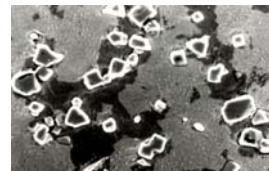
Optical absorption in photonic crystals of potassium acid phthalate has been measured at room temperature, from which the band gap has been determined and the optical band gap was calculated by using absorption spectrum. The analysis of absorption coefficient in the absorption region reveals a direct band gap of 3.70 eV. Further this study includes the theoretical calculations to determine the optical constant of the material and a technique for photonic band gap tuning which is ...



Page **674–678** \_\_\_\_\_ K. I. Parashivamurthy, P. Sampathkumaran, and S. Seetharamu

### In-situ TiC precipitation in molten Fe-C and their characterisation

TiC particles were formed in liquid iron solution by the reaction between pure titanium and carbon available in molten iron. TiC particles have been precipitated in steels with four different carbon contents by *in situ* reactions during melting. The influence of titanium and carbon concentration on the precipitation of TiC was ...



Page **679–682** \_\_\_\_\_ S. Kar and K. S. Bartwal

### Reduction of domain wall width in VTE treated near stoichiometric LiNbO<sub>3</sub> crystals

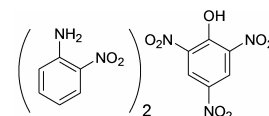
LiNbO<sub>3</sub> is a ferroelectric crystal and grows with multi domains. Different domains are separated by boundaries which are known as domain boundaries. Domain walls for congruent and VTE (Vapor Transport Equilibration) treated near stoichiometric lithium niobate samples were visualised in different crystallographic directions using chemical etching technique. The sample is ...



Page **683–688** \_\_\_\_\_ R. Bharathikannan, A. Chandramohan, M. A. Kandhaswamy, J. Chandrasekaran, R. Renganathan, and V. Kandavelu

### Synthesis, crystal growth and properties of the charge transfer complex adduct of 2-nitro aniline with picric acid – An organic non-linear optical material

The organic NLO material 2-nitro aniline and picric acid (2NAP) was synthesized, needle shaped single crystals of dimension  $10 \times 1 \times 0.8 \text{ mm}^{-3}$  were grown by slow evaporation solution growth technique from the saturated solution of the title compound in chloroform at ...



Crystal Research and Technology is indexed in Cambridge Scientific Abstracts, CCR Database, Chemical Abstracts Service/SciFinder, ChemInform, Chemistry Citation Index™, Chemistry Server Reaction Center, Chimica Database, COMPENDEX, CSA Technology Research Database, Current Contents®/Physical, Chemical & Earth Sciences, FIZ Karlsruhe Databases, INSPEC, Journal Citation Reports/Science Edition, Materials Science Citation Index®, Reaction Citation Index™, Science Citation Index Expanded™, Science Citation Index®, SCOPUS, VINITI, Web of Science®